Behaviour of a portion of railway track under maintenance operation

T.M.P. Hoang[1], G. Saussine[1], D. Dureisseix[2], P. Alart[3]
[1]SNCF, Paris, France
[2]LaMCoS, INSA de Lyon, France
[3]LMGC, Université Montpellier II, France
{thi-minh-phuong.hoang,gilles.saussine}@sncf.fr
david.dureisseix@insa-lyon.fr
Pierre.Alart@univ-montpe2.fr

Abstract

The track deterioration rate is strongly influenced by the ballast behaviour under tra□c. In order to restore the initial track geometry, di□erent maintenance processes are performed, like tamping, dynamic stabilisation. A better understanding of the ballast behaviour under these operations on a portion of railway track is a key to optimize the process, to limit degradation and to propose some concept for a better homogeneous compaction. In this work, we focus on the study of tamping process over several sleepers by the numerical simulation using the Non-Smooth Contact Dynamics (NSCD) of three-dimensional Discrete Element Method (DEM) simulations improved by a Domain Decomposition Method and Parallel Computation.

Keywords: Railway ballast, Tamping process, Discrete Element Method, Non-Smooth Contact Dynamics (NSCD), Domain Decomposition Method, Parallel Computation.

Introduction

Ballast is the major support element of the railway track. It must fulfill not only the high permeability for rapid drainage, but also the high sti□ness for e□ciently spreading train loads over the sub-base.

However, under the repeated heavy train loading, the ballast particles rearrange, degrade and provoke at a long term a settlement of the track, which is often inhomogeneous. This has been identified as the main cause of loss of track geometry and subsequently make a loss in ride quality of the track. For the high speed trains, the passenger is more sensitive to ride quality deterioration, thus the maintenance operation is more frequently required.

One of the permanent maintenance operations is tamping. This process is used to restore the correct geometrical position, i.e the initial profile of the ballasted track. It is peformed by a ballast tamper or a tamping machine which works by vibrating the ballast and pushing it under the sleeper. In order to increase the e□ciency, to reduce the cost, the duration of the tamping process, and to ensure the safety of the high speed line, we propose herein a detailed study of the mechanical behaviour of the ballast during tamping.

Currently, laboratory testing and numerical simulations are known as two principal research actions to investigate the mechanical behaviour of ballast. For such a purpose, the second way is chosen and developed in this article. In this framework, Non-Smooth Contact Dynamics (NSCD) of three-dimensional Discrete Element Method (DEM) simulations improved by Domain Decomposition Method performed with the Shared Memory parallel technique (using OpenMP) has been applied to the granular mechanics as the ballast media. In principle, the domain of the problem is split geometrically into subdomains, and treated simultaneously by several processors.

The original results concern a simulation of a more realistic railway track portion composed of 7 sleepers, submitted to a tamping process. This numerical simulation requires about 90000 three-dimensional polyhedral digitized ballast grains. The post-processing analysis shows the influence of the tamping process from one sleeper to another sleeper in terms of compaction and local mechanical indicators.

Tamping process

Tamping is performed by a ballast tamper, which restores the correct geometrical position of the

ballasted track, improves the compactness of the ballast below the areas near the rail, and achieves a more confortable ride for passengers and freight. A tamping machine consists of tamping units, one of which is provided with four pairs of tamping tools (arms or ”tines”). These pairs are distributed to tamp each side of the sleepers, its number depends on the machine, for example 16 tampings tines for a single sleeper, 32 tines for two sleepers,...

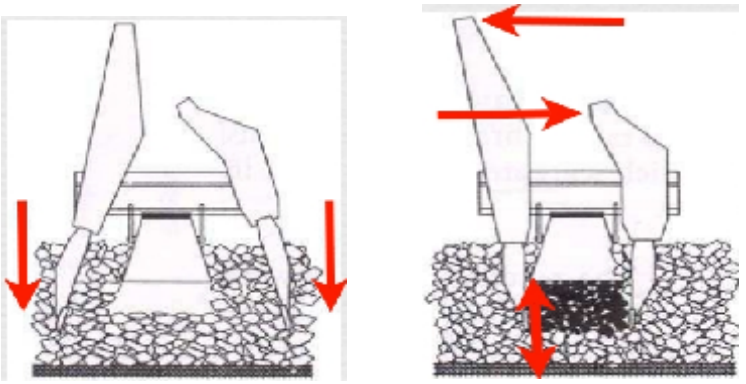

Figure 1: Tamping tines squeeze the ballast under the sleeper ([3])

Tamping whole procedure takes just a few seconds and is known as the Tamping Cycle. The cycle itself has three steps: (1) penetration, (2) squeezing, and (3) moving ([3], [4]):

• *(1) Penetration phase*: first, the track is lifted, next, the tamping tines oscillate enough quickly to break the surface of the ballast, and simultaneously penetrate into the ballast on either side of the sleeper. This phase contributes to 50 % of the final compaction gain of the zone under the sleeper [3]. Therefore, in order to get the best result from this tamping action, the vibration frequency and the penetration depth have to be carefully chosen. In fact, the vibration frequency varies between 35 Hz and 45 Hz according to constructors, and the tines are set a distance from 15 mm to 20 mm below the bottom side of the sleeper.

• *(2) Squeezing phase*: the tamping tines squeeze the ballast under the sleeper and pack it together. In general, the tool tamp the ballast only below the areas near the rail, while the space between the rails isn’t necessarily tamped. The reasons for this are quite practical. First, the area below the rail requires the most support. Secondly, if ballast is mechanically tamped along the full length of the sleeper, the ballast below the center of the sleeper will eventually become more compacted with the passage of trains. Then, under the weight of the train, the sleeper will rock back and forth, in extreme situations, the sleeper can break in the middle, [2]. In this phase, for the best e□ect, we hold attention for the squeezing vibration frequency, the squeezing force, the squeezing time. Normally, its values varies between 35 − 45 Hz , 16 − 19 kN and 0, 8 − 1 s.

• *(3) Moving phase (Lifting phase)*: the tamping tines are lifted and the machine is moved to the next sleeper to repeat the cycle. In fact, in order to make the lift easier, the tines have the free movements in the squeezing direction during the lifting phase. However, this provokes a loss of compaction under the sleeper. On the other side, the compaction due to this phase maybe gained by freezing the movement of the tamping tool in the squeezing direction during the lift (i.e. the pressure in the squeezing direction is maintained).

In order to improve the quality of the tamping process, it’s necessary to analyze the influence of tamping parameters and chose its best values. A such study is proposed in [1].

Numerical methods

The NSCD method is based on a particle-scale model of granular dynamics with two major ingredients: the dynamics equation and the contact law. In this framework, the system is assumed to be a collection of rigid bodies submitted to external e□orts and non-smooth interaction such as contact and friction. The detailed method principle is presented in [11].

Domain Decomposition Method (DDM)

Geometrical partitioning principle :

For the case of large-scale problems, a partitioning strategy belonging to the Domain Decomposition Method (DDM) is selected. In this framework, the granular system is considered as sets of nodes (grains) and links (potential contact interactions detected at a particular time step), see figure. 2.

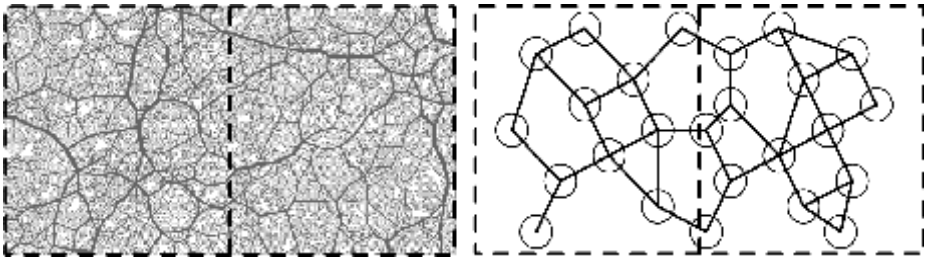

Figure 2: Box-decomposition of a 2D granular media (left) and its principle (right) ([5])

If a graph is defined with nodes as vertices, and links as edges, the nodes can be split among the subdomains (considering their center of mass coordinates). The figure 3 shows a detailed partitioning description. The links are located on subdomains if its two consisting nodes belong to the same subdomains; on the contrary, the links constitute a global interface if they are the interactions between two nodes belonging to di□erent subdomains.

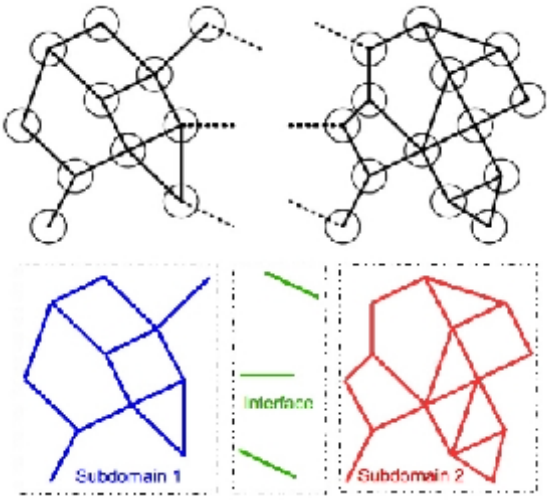

Figure 3: Decomposition principle: links on global interface and on subdomains ([9])

The subdomains are treated as granular systems coupled with its neighbours by specific boundary conditions arising from a global interface. For the remaining side, the global interface is considered as a particular subdomain in which exist only the links and no node is dealt.

Algebraic partitioning principle :

An algebraic partitioning principle is constructed for according to its theory. For sake of simplicity, the subscript E , E' , Γ denote in the following subdomains and the global interface; the capital and small letters represent respectively the grain level variables and the contact level variables. The grain velocity, the internal interaction impulses are defined by:

$$V = \begin{bmatrix} V_E \\ V_{E'} \end{bmatrix} \qquad \text{and} \qquad R = \begin{bmatrix} R_E \\ R_{E'} \end{bmatrix} \tag{1}$$

Similarly, the relative velocities and the interaction impluses are split as:

$$v = \begin{bmatrix} v_E \\ v_{E'} \\ v_\Gamma \end{bmatrix} \qquad \text{and} \qquad r = \begin{bmatrix} r_E \\ r_{E'} \\ r_\Gamma \end{bmatrix} \tag{2}$$

The dynamical evolution of the grains on the subdomain E is therefore:

$$M_E V_E = M_E V_E^i + R_E^d + R_E + R_{E\Gamma} \tag{3}$$

where M_E represents the mass and inertia matrix, V^i_E, respectively V_E denote the velocities at the time step t_i , respectively t_{i+1} , R^d_E is the external impulsions, l'index EΓ informs the impulse of Γ acting on E,

$$R_E = H_E r = h_E r_E \qquad \text{and} \qquad R_{E\Gamma} = H_{E\Gamma} r = h_{E\Gamma} r_\Gamma \tag{4}$$

and,

$$v_E = H_E^T V = h_E^T V_E \qquad \text{and} \qquad v_\Gamma = \sum_E H_{E\Gamma}^T V = \sum_E h_{E\Gamma}^T V_E \tag{5}$$

Note that since each subdomain is independent from each other, the block decomposition of H (the global-to-local operator) and its transpose H^T into h, h^T can be used. $W = H^T.M^{-1}.H$ is also called the Delassus operator.

The condensed dynamics on each subdomain and interface leads to an algebraic splitting of the reference problem:

$$\begin{bmatrix} v_E \\ v_{E'} \\ v_\Gamma \end{bmatrix} = \begin{bmatrix} v_E^d \\ v_{E'}^d \\ v_\Gamma^d \end{bmatrix} + \begin{bmatrix} W_E & 0 & W_{E\Gamma} \\ 0 & W_{E'} & W_{E'\Gamma} \\ W_{\Gamma E} & W_{\Gamma E'} & W_\Gamma \end{bmatrix} \begin{bmatrix} r_E \\ r_{E'} \\ r_\Gamma \end{bmatrix} \tag{6}$$

where

$$\begin{aligned} v_E^d &= h_E^T (V_E^i + M_E^{-1} R_E^d) \\ v_\Gamma^d &= \sum_E h_{E\Gamma}^T (V_E^i + M_E^{-1} R_E^d) \\ W_E &= h_E^T M_E^{-1} h_E \\ W_{E\Gamma} &= W_{\Gamma E}^T = h_E^T M_E^{-1} h_{E\Gamma} \end{aligned}$$

and

$$W_\Gamma = \sum_E h_{E\Gamma}^T M_E^{-1} h_{E\Gamma} \tag{7}$$

According to this algebraic formulation, the DDM leads to a parallel version for reducing the simulation time. The subdomains are treated simutaneously by di□erent processors, specially the global interface is addressed in a specific step to provide a synchronized algorithm.

DDM-OpenMP algorithm

The corresponding generic program is described in the following algorithm. This algorithm is suited to a Shared Memory parallelization via compilation directives (typically, OpenMP). In fact, we choose this parallel technique because of its lower intrusive characteristic in the implementation platform.

Algorithm 1 DDM–OpenMP–NLGS

```
Loop on time steps
for i = 1, 2... do
  Gap prediction and potential contact detection
  Domain partitioning
  Parallel loop on subdomains
  for E − 1, 2... n_SD do
    Compute free velocities per subdomain E
  end for
  Loop on DDM iterations
  for j = 1, 2... n_DDM do
    Parallel loop on subdomains
    for E = 1, 2... n_SD do
      NLGS resolution per subdomain E, with n sweeping iterations
      Compute error contribution of subdomain E
    end for
    NLGS resolution on global interface Γ, with m sweeping iterations
    Compute error contribution of interface Γ
    Assemble error contributions, to check for loop termination
  end for
  Parallel loop on subdomains
  for E − 1, 2... n_SD do
    Compute nodal quantities (velocities and position updates)
  end for
end for
```

Results

Note that the simulation of tamping process is an application case requiring a gain of computing time to perform an extensive parametric study. Moreover, we focus herein on the behaviour of a ballasted track submitted to a maintenance operation. For this, a three-dimension sample with 3.6 m × 2 m × 0.56 m is constructed to represent a real track slice submitted to a tamping cycle.

The proposed test case concerns a slice of a ballasted railway with 7 sleepers submitted to a tamping cycle on the fourth sleeper (three first sleepers have been already tamped). Figure 4 illustrates the initial state. For each phase of tamping cycle, we apply:

- a penetration speed of 1.6 m/s, a vibration frequency of 35 Hz in 0.2 s,
- a squeezing vibration frequency of 35 Hz , a squeezing force of 6 kN in 1.2 s,
- a lifting speed of 1 m/s and a vibration frequency of 35 Hz in 0.36 s.

The modelling sample contains 88 100 ballast grains (polyhedra) and an average of 310 000 frictional contact interactions. The grains are in contact between itselfs, also with sleepers and tamping tines, with a friction coe□cient μ = 1. There are 5 planes delimiting the sample, each with a friction coe□cient μ = 0.8.

According to a previous study, the parameters are fixed as follows:

- time interval [0,T] with T = 1.764 s discretized in 8820 time steps,
- 7 subdomains under the seven sleepers (n_{SD} = 7 ⇔ domain is split according to the x, y, z axis into 1 × 7 × 1 subdomains and 1 global interface),
- 740 DDM iterations (n_{DDM} = 740),
- 1 sweeping iteration (Non-Linear Gauss-Seidel iteration: n_{NLGS} = n = m = 1).

The computation is performed on a 2 Dual-Core processor machine, i.e. with a resource of a maximum of 4 processors. The results are analyzed in terms of physical quantity of interest for the ballast as compactness, and also its compaction gain.

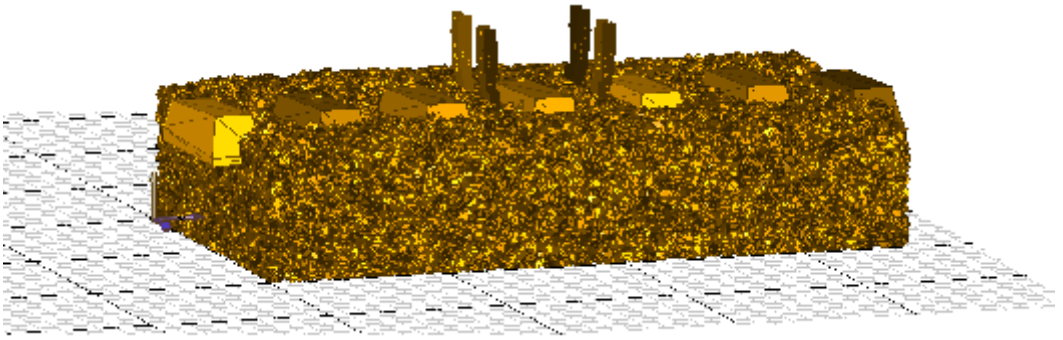

Figure 4: Sample in 3D representative of one slice of a ballasted railway with 7 sleepers submitted to a tamping cycle on the fourth sleeper (7 sleepers are successively numbered and tamped from left to right. In detail, three sleepers on the left have been already tamped.)

The compactness allows to define that a sample is dense or loose; similarly, it is the solid fraction of the sample, identified by the ratio between the sum of the volumes of the grains in the sample and the total volume of the sample. Figure 5 shows the compactness evolution of a zone under the sleeper 4. We observe distinctly three phases of tamping cycle and also the di□erent variation of compactness during the process which is detailed in the following:

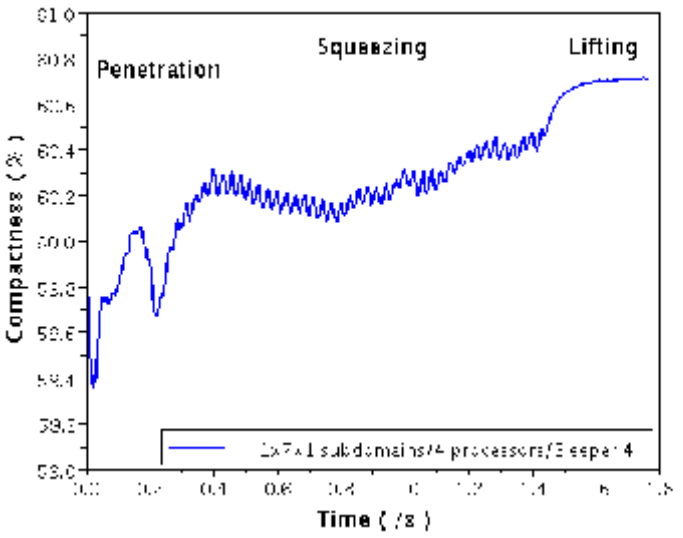

Figure 5: Compactness evolution of a zone under the fourth sleeper obtained by the DDM-OpenMP test.

• *In the penetration phase*: a compaction fall occurs at the beginning of phase. The lift of the track is a cause. Moreover, the tamping process on the sleeper 3 makes the grains around the sleeper 4 unstable, this provoke a rearrangement as soon as the tamping tines begin its task.

• *In the squeezing phase*: the compactness decreases a lot at the start, then fluctuates and increases up to the end of phase. Note that the lift of tamping tines on the sleeper 3 creates voids between the third and the fourth sleeper, so the left tines (beside the sleeper 3) penetrate more easily than the right tines (beside the sleeper 5). And with the vibration action, this takes a displacement flux of the grains below the sleeper which is left – right asymmetric. Therefore, we have a significative compaction loss at the beginning of phase. From beginning to the moment t_s = 0.8s, the asymmetry is still present, that perturbs the

grain movement and cause a light compaction diminution at the mi-term. However, from the moment t_s = 0.8s, the displacement field becomes symmetric under the squeezing action and provides a compaction gain at the end of phase.

• *In the lifting phase*: we obtain an additional compaction gain in this phase. The pressure in the squeezing direction is maintained during the lift by freezing the movement between the tines. This contributes to re-compact the ballast.

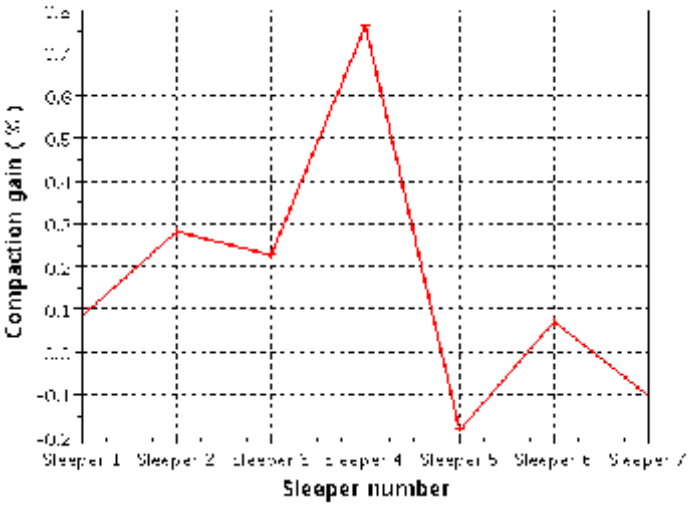

Figure 6: The final compaction gain of zones under 7 sleepers after a tamping cycle applied to the fourth sleeper.

The final compaction gain of all the zones under 7 sleepers are given in the Figure 6. The region under the fourth sleeper has certainly the most great gain about of 0.8% after it is tamped. Furthermore, the tamping cycle on the sleeper 4 a□ects eventually its neighbours, for instance: an additional compaction gain of the regions on the left which have been already tamped, and a compaction loss of the regions on the right. That means the cycle submitted to the fourth sleeper favours the re-compaction on the left, on the contrary, it provoke an unfavourable reorganization on the right.

Conclusions

The behaviour of a portion of ballasted track under the tamping process was investigated above in term of compactness and compaction gain. These parameters are crucial to propose orientations to decrease maintenance cost. This post-processing study is performed by the numerical simulation using the Non-Smooth Contact Dynamics (NSCD) as a three-dimensional Discrete Element Method (DEM) improved by a Domain Decomposition Method and Parallel Computation. These approaches allow to decrease the computation time, in detail: we obtain in this case a computation time of 7860 minutes in parallel with 4 processors versus 14019 minutes for a sequential run (PC Dual-Core 8Go RAM).

In conlusion, we remark that the development of numerical methods proposed in this paper allows to not only get a better understanding of the track behaviour in the moderate time, but also in the long-term to treat larger problems. Indeed, the full industrial tamping process perfomed automatically on a portion of ballasted track simuled by a larger number of processors on a multicore environment is expected.

Acknowledgement

All simulations are performed with the OpenSource LMGC90 platform ([6]) (http://www.lmgc.univ-montp2.fr/dubois/LMGC90). The authors acknowledge sincerely F. Dubois and LMGC90 team from Laboratoire de Mécanique et de Génie Civil de l'Université Montpellier 2 (France).

References

[1] R. Perales, G. Saussine, N. Milesi, F. Radjai, *Tamping Process Optimization*.

[2] B. Solomon, *Railway maintenance*, P.79 - P.82, MBI Publishing Company, 2001, USA.

[3] E.Azéma, *Etude numérique des matériaux granulaires à grains polyédriques: rhéologie quasi-statique, dynamique vibratoire, application au procédé de bourrage du ballast*, thesis, 19 October 2007.

[4] C. Paderno, *Comportement du ballast sous l'action du bourrage et du trafic ferroviaire*, Phd EPFL 2010.

[5] L. Champaney, D. Dureisseix, *A mixed domain decomposition approach, in Mesh Partitioning Techniques and Domain Decomposition Methods*, F. Magoulès ed, Civil-Comp Press, 293-320, 2007.

[6] F. Dubois, M. Renouf, *Numerical strategies and software architecture dedicated to the modelling of dynamical systems in interaction. Application to multibody dynamics*, ECCOMAS Thematic Conference, Milano, Italy, 25-28 June 2007.

[7] M. Renouf, *Optimisation numérique et calcul parallèle pour l'étude des milieux divisés bi- et tridimensionnels*, thesis, 14 Septembre 2004.

[8] S. Nineb, P. Alart, and D. Dureisseix. *Domain decomposition approach for nonsmooth discrete problems, example of a tensegrity structure*. Computers and Structures, 85(9):499-511, 2007.

[9] P. Alart, D. Dureisseix, T.M.P Hoang, G. Saussine, *Domain Decomposition methods for granular dynamics using discrete elements and application to railway ballast*, 7th Meeting Unilateral Problems in Structural Analysis, Palmanova June 17-19 2010.

[10] G. Saussine, *Contribution à la modélisation de granulats tridimensionnels: Application au ballast*, thesis, 14 October 2004.

[11] B. Cambou, M. Jean. *Micromécanique des matériaux granulaires*, HERMES Science Europe Ltd, 2001.